

Optimal observables for Z' models in annihilation leptonic processes

A. V. Gulov* and Ya. S. Moroz

Dnipro National University, 49010 Dnipro, Ukraine



(Received 26 January 2018; published 10 December 2018)

The optimal observables with the best ratio of signal to statistical uncertainty are proposed for a bunch of popular models of the Z' boson. They are the cross sections integrated over the phase space of the final particles with proper weight functions. It is shown that the proposed observables are completely equivalent to the χ^2 fit of the differential cross section, so they could be used as an alternative of aggregating events into bins with further minimization of the χ^2 function, especially in preliminary analysis of experimental data. Application of the observables to the maximum likelihood estimate of the Z' mass and the Z - Z' mixing angle as well as to the exclusion reach and statistical efficiency of the signal is investigated in details.

DOI: [10.1103/PhysRevD.98.115014](https://doi.org/10.1103/PhysRevD.98.115014)

I. INTRODUCTION

The International Linear Collider (ILC) is discussed in the literature as a future experiment in high-energy physics [1]. This engine is expected to collide partially polarized electrons and positrons at the center-of-mass energies up to 1 TeV. The ILC will allow performing precise tests of the Standard Model (SM) and beyond, being a natural perspective for the current experiments on the CERN LHC. The combined analysis of future data from the ILC with the data obtained at the LHC is also a point of interest (e.g., see Ref. [2]).

Searches for new particles beyond the SM is one of the basic parts of the ILC experimental program. In this paper, we focus on the Z' boson arising in a bunch of popular models. We consider the $e^+e^- \rightarrow \mu^+\mu^-$ process with the simplest annihilation kinematics at the center-of-mass energies 250 GeV, 500 GeV, and 1 TeV. Taking into account the actual bounds on the Z' mass (~ 4 TeV) derived from various experiments [3,4], we conclude that the energy of collisions at the ILC will be significantly below the Z' resonance. This means the Z' boson could manifest itself through tiny contact couplings between fermionic currents induced by intermediate Z' virtual states. Therefore, amplification of the corresponding signal is of great interest.

Usual observables, such as the total cross section σ_T and the forward-backward asymmetry A_{FB} , might be essentially

upgraded to increase statistical resolution as much as possible. To achieve the goal, we propose an observable constructed by integration of the differential cross section over the scattering angle with a properly chosen weight function. Such a scheme generalizes the idea of well-known forward-backward or center-edge cross sections based on steplike weights for different scattering angles. In our approach, the weight function is calculated to reach the strongest Z' signal with respect to the statistical noise. The corresponding integrated cross section is called *the optimal observable*. In a model-independent approach, amplification of signals of the Z' boson by means of the weighted integrated cross section was discussed in Ref. [5].

The optimal observables are known in the high-energy physics, although they are unfortunately paid no attention in searching for the Z' boson. They were initially applied to the analysis of the magnetic and electric dipole moments of the t quark [6] and to the measurement of triple gauge boson couplings at the CERN Large Electron-Positron Collider [7,8]. The recent usage of the optimal observables is the investigation of the CP invariance in vector-boson fusion production of the Higgs boson at the LHC [9]. The optimal observables were actually rediscovered in Ref. [5]. So, the present paper could be also considered as an introduction to the optimal observables in application to the Z' boson phenomenology. The resulting weight functions to integrate the differential cross section coincides with the general theory given in Refs. [6,7].

We will discuss that the optimal observable is an equivalent replacement of the χ^2 fit of the differential cross section. This means that there is a unique weight function in the phase space to integrate the cross section without losses of information encoded in the differential cross section. In other words, instead of collecting events into

*alexey.gulov@gmail.com

Published by the American Physical Society under the terms of the [Creative Commons Attribution 4.0 International license](https://creativecommons.org/licenses/by/4.0/). Further distribution of this work must maintain attribution to the author(s) and the published article's title, journal citation, and DOI. Funded by SCOAP³.

bins and further χ^2 analysis, all the events could be summed up directly with the predefined weights dependent on the scattering angle. This gives a signal of the highest quality allowed by the luminosity. So, the proposed scheme might be considered as a convenient alternative of the analysis of the differential cross section in searches for the Z' boson. Moreover, it can be applied even in the case in which the statistics is not rich enough to collect and publish the differential cross section.

Many models of the “new physics” beyond the SM have been developed, and the Z' boson is a usual ingredient of them. In practical searches for the Z' boson, a pool of models is traditionally selected. The earlier set included the models related to different branches of the grand unification theory based on the E_6 gauge group [10–13]. Then, it was enlarged by the alternative left-right model, the littlest Higgs model, etc. At the moment, the LHC collaborations discuss about ten Z' models in data analysis. We consider the models discussed in the ILC Technical Design Report [1] and some others:

- (i) In the *sequential Standard Model* (SSM), the Z' couplings to fermions coincide with the SM Z couplings. There is no unification of interactions in this test model. However, it is useful to clarify the definitions of Z' couplings.
- (ii) E_6 *models* [14] are based on the gauge breaking scheme $E_6 \rightarrow \text{SO}(10) \times \text{U}(1)_\psi \rightarrow \text{SU}(5) \times \text{U}(1)_\chi \times \text{U}(1)_\psi \rightarrow \text{SU}(3)_C \times \text{SU}(2)_L \times \text{U}(1)_Y \times \text{U}(1)_{\theta_{E_6}}$. The model contains a free parameter: the mixing angle β between the ψ and χ symmetry states. The angles $\beta = 0, \pi/2$ and $\arctan(-\sqrt{5/3})$ correspond to the models called χ, ψ , and η .
- (iii) The *left-right model* (LR) [15] is related to the gauge breaking scheme $\text{SO}(10) \rightarrow \text{SU}(3)_C \times \text{SU}(2)_L \times \text{U}(1)_Y \times \text{U}(1)_\chi \rightarrow \text{SU}(3)_C \times \text{SU}(2)_L \times \text{SU}(2)_R \times \text{U}(1)_{B-L}$. There is a free model parameter $\sqrt{2/3} \leq \alpha \leq \sqrt{c_W^2/s_W^2 - 1}$. The minimal value $\alpha = \sqrt{2/3}$ coincides with the χ model. The maximal value $\alpha = \sqrt{c_W^2/s_W^2 - 1}$ corresponds to the *left-right symmetric model* (LRS).
- (iv) The *alternative left-right model* (ALR) [16] provides the gauge breaking scheme $\text{SO}(10) \rightarrow \text{SU}(3)_C \times \text{SU}(2)_L \times \text{U}(1)_Y \times \text{U}(1)_\chi \rightarrow \text{SU}(3)_C \times \text{SU}(2)_L \times \text{SU}(2)_R \times \text{U}(1)_{B-L}$. The ALR model is also discussed in Ref. [17].
- (v) The *littlest Higgs model* (LH) [18] considers the gauge breaking scheme $\text{SU}(5) \rightarrow [\text{SU}(2)_1 \times \text{U}(1)_1] \times [\text{SU}(2)_2 \times \text{U}(1)_2] \rightarrow \text{SU}(2)_L \times \text{U}(1)_Y$. The model is also discussed in Ref. [19].
- (vi) The *simplest little Higgs model* (SLH) [20] is based on the gauge breaking scheme $\text{SU}(3)_w \times \text{U}(1)_X \rightarrow \text{SU}(2)_w \times \text{U}(1)_Y$. Two alternatives are proposed within the model: the *universal SLH* (USLH) and the *anomaly-free SLH* (AFSLH). However, both the

alternatives lead to equal leptonic couplings. The model is also discussed in Ref. [21].

- (vii) The $\text{U}(1)_X$ *model* [22] was introduced recently as a minimal $\text{U}(1)$ extension of the SM with conformal invariance at the classical level. We choose the Z' coupling and the free model parameters in accordance with Ref. [23], which ensures the vacuum stability in the model.

In every Z' model mentioned, the Z' couplings are known, whereas the Z' mass and the Z – Z' mixing angle remain arbitrary parameters to be fitted in experiment. The Z – Z' mixing angle is bounded experimentally at least as $|\sin \theta_0| < 10^{-3}$ [24] and usually neglected in data analysis [1,10–13,25]. In this paper, we discuss the Z – Z' mixing separately.

The paper is organized as follows. In Sec. II, we consider the differential cross section of the $e^+e^- \rightarrow \mu^+\mu^-$ process and group the Z' models into four different pools in dependence on the Z' couplings to leptons. In Sec. III, the optimal observable for the Z' signal is derived as an analytic solution by maximization of the signal-to-uncertainty ratio. In Sec. IV, we show that the optimal observable is equivalent to the χ^2 fit of the differential cross section and can be used to derive confidential intervals for the Z' parameters. Effects of the Z – Z' mixing are considered in detail in Sec. V. In the discussion section, we estimate the exclusion reach for the Z' mass and compare the optimal observables with the popular approach of data fitting based on the forward-backward asymmetry.

II. DIFFERENTIAL CROSS SECTIONS

The expected scale of the grand unification as well as the Z' mass is much larger than the ILC center-of-mass energies. So, the Z' boson phenomenology at the ILC can be described by contact interactions between fermionic currents. We use the Lagrangian of neutral currents in the standard notations [10–13,17,19,21],

$$\begin{aligned}
 -L_{NC} &= eA_\beta J_{A,\beta} + g_Z Z_\beta J_{Z,\beta} + g_{Z'} Z'_\beta J_{Z',\beta}, \\
 J_{A,\beta} &= \sum_f \bar{f} \gamma^\beta v_f^{(0)} f, \\
 J_{Z,\beta} &= \sum_f \bar{f} \gamma^\beta (v_f - \gamma_5 a_f) f, \\
 J_{Z',\beta} &= \sum_f \bar{f} \gamma^\beta (v'_f - \gamma_5 a'_f) f,
 \end{aligned} \tag{1}$$

where all the SM fermions f appear in the sum, A is the photon, Z is the SM neutral vector boson, Z' is the new heavy neutral vector boson, $e = \sqrt{4\pi\alpha_{em}}$ is the positron charge, g_Z and $g_{Z'}$ are the couplings to the corresponding boson (see Table I, $g_Z = g_{Z',\text{SSM}}$), $v_f^{(0)}$ is the fermion electric charge in e units, v_f and a_f are the vector and axial-vector coupling of the fermion to the Z boson, and v'_f

TABLE I. The Z' coupling in the models. The cosine and sine of the Weinberg angle are denoted by c_W, s_W .

	$g_{Z'}$
SSM	$e/(s_W c_W)$
E_6, LR	e/c_W
ALR	$e/(s_W c_W \sqrt{1 - 2s_W^2})$
LH	e/s_W
USLH, AFSLH	$e/(c_W \sqrt{3 - 4s_W^2})$
$U(1)_X$	$e/(4c_W)$

and a'_f are the couplings to the Z' boson. The Z' boson couplings are collected in Table II.

The differential cross section of the process $e^+e^- \rightarrow \mu^+\mu^-$ consists of the SM part and the Z' contribution. Since we assume the energies significantly below the threshold of Z' decoupling, $\sqrt{s} \ll M_{Z'}$, it can be expanded by a small parameter,

$$\frac{d\sigma}{dz} = \frac{d\sigma^{\text{SM}}}{dz} + \sum_{n=1}^{\infty} \mu^n F_n(s, z, a', v'), \quad (2)$$

$$\mu = \frac{M_Z^2}{s - M_{Z'}^2}, \quad (3)$$

where z is the cosine of the scattering angle of the charged lepton in the center-of-mass frame, M means the mass of the corresponding particle, F are factors measured in the same units as the cross section, and \sqrt{s} is the center-of-mass energy. The magnitude of the expansion parameter μ is about 10^{-4} for $\sqrt{s} = 1$ TeV and $M_{Z'} = 4$ TeV. Heavier Z' masses and lower collision energies give smaller μ . As is seen, the Z' mass, measured in units of M_Z , plays the role of an unknown dimensionless parameter of the model, whereas other components of (2) can be calculated numerically. We neglect the widths of vector bosons, since they are a few percent of the boson mass in the considered models and the energies are aside from the Z and Z' peaks.

In our paper, the SM differential cross section is calculated by two complementary approaches. First, we use FEYNARTS [26], FORMCALC [27], and LOOPTOOLS [27] up to one-loop radiative corrections for the weak sector. Effects of the quantum electrodynamics is taken into account in accordance with Ref. [28]: the soft photon bremsstrahlung is included analytically, whereas the hard photon bremsstrahlung is included by numerical integration in the phase space of the final state. The domain in the phase space is determined by the event selection rule $\sqrt{s'}/s > 0.85$, where s' is the Mandelstam variable of the final pair $\mu^+\mu^-$ and s is the Mandelstam variable of the final state with the photon $\mu^+\mu^-\gamma$. Second, the SM differential cross section is computed by ZFITTER software [29]. The discrepancy between the results is less than 2%. So, we

TABLE II. The Z' couplings to fermions. The sine of the Weinberg angle is denoted by s_W . For the E_6 models, $A = \frac{\cos\beta}{2\sqrt{6}}$, $B = \frac{\sqrt{10}\sin\beta}{12}$. The special values of the mixing angle $\beta = 0, \pi/2$, and $\arctan(-\sqrt{5/3})$ correspond to χ, ψ , and η models. In the LR model, $\sqrt{2/3} \leq \alpha_{LR} \leq \sqrt{c_W^2/s_W^2 - 1}$. The LRS model corresponds to $\alpha = \sqrt{c_W^2/s_W^2 - 1}$. The LH model includes the parameter $\frac{1}{10} \leq \frac{c}{s} \leq 2$, and we choose $\frac{c}{s} \equiv 1$ [19]. In the $U(1)_X$, we choose $x_\Phi = 2$ and $x = x_H/x_\Phi = 1$ or -1.25 .

f	ν	e	u	d
SSM				
$2v'_f$	$\frac{1}{2}$	$2s_W^2 - \frac{1}{2}$	$\frac{1}{2} - \frac{4}{3}s_W^2$	$\frac{2}{3}s_W^2 - \frac{1}{2}$
$2a'_f$	$\frac{1}{2}$	$-\frac{1}{2}$	$\frac{1}{2}$	$-\frac{1}{2}$
E_6				
$2v'_f$	$3A + B$	$4A$	0	$-4A$
$2a'_f$	$3A + B$	$2(A + B)$	$2(B - A)$	$2(A + B)$
LR				
$2v'_f$	$\frac{1}{2\alpha}$	$\frac{1}{\alpha} - \frac{\alpha}{2}$	$\frac{\alpha}{2} - \frac{1}{3\alpha}$	$-\frac{1}{3\alpha} - \frac{\alpha}{2}$
$2a'_f$	$\frac{1}{2\alpha}$	$\frac{\alpha}{2}$	$-\frac{\alpha}{2}$	$\frac{\alpha}{2}$
ALR				
$2v'_f$	$s_W^2 - \frac{1}{2}$	$\frac{5}{2}s_W^2 - 1$	$\frac{1}{2} - \frac{4}{3}s_W^2$	$\frac{1}{6}s_W^2$
$2a'_f$	$s_W^2 - \frac{1}{2}$	$-\frac{1}{2}s_W^2$	$s_W^2 - \frac{1}{2}$	$-\frac{1}{2}s_W^2$
LH				
$2v'_f$	$\frac{c}{4s}$	$-\frac{c}{4s}$	$\frac{c}{4s}$	$-\frac{c}{4s}$
$2a'_f$	$\frac{c}{4s}$	$-\frac{c}{4s}$	$\frac{c}{4s}$	$-\frac{c}{4s}$
USLH				
$2v'_f$	$\frac{1}{2} - s_W^2$	$\frac{1}{2} - 2s_W^2$	$\frac{1}{2} + \frac{1}{3}s_W^2$	$\frac{1}{2} - \frac{2}{3}s_W^2$
$2a'_f$	$\frac{1}{2} - s_W^2$	$\frac{1}{2}$	$\frac{1}{2} - s_W^2$	$\frac{1}{2}$
AFSLH				
$2v'_f$	$\frac{1}{2} - s_W^2$	$\frac{1}{2} - 2s_W^2$	$-\frac{1}{2} + \frac{4}{3}s_W^2$	$\frac{1}{3}s_W^2 - \frac{1}{2}$
$2a'_f$	$\frac{1}{2} - s_W^2$	$\frac{1}{2}$	$-\frac{1}{2}$	$s_W^2 - \frac{1}{2}$
$U(1)_X$				
$2v'_f$	$-x_H - x_\Phi$	$-3x_H - x_\Phi$	$\frac{5}{3}x_H + \frac{1}{3}x_\Phi$	$-\frac{1}{3}x_H + \frac{1}{3}x_\Phi$
$2a'_f$	$-x_H$	x_H	$-x_H$	x_H

add 2% systematic error to the SM differential cross section obtained in the first approach (Fig. 1). This systematic error covers also four-fermion final states with leptons missed in the beams, the contribution of which is estimated to be less than 1% [5].

The leading-order (LO) Z' factor F_1 in (2) arises from the interference between the SM amplitude and the Z' exchange amplitude. For our purposes, it is calculated in the improved Born approximation with the running constants. The factor can be written in the form

$$F_1(s, z, a', v') = \frac{\alpha_{\text{em}} g_{Z'}^2}{32 \sin^2 \theta_W \cos^2 \theta_W M_{Z'}^2} \times \left[z f(s, a'_e, v'_e) + \frac{1+z^2}{2} f(s, v'_e, a'_e) \right], \quad (4)$$

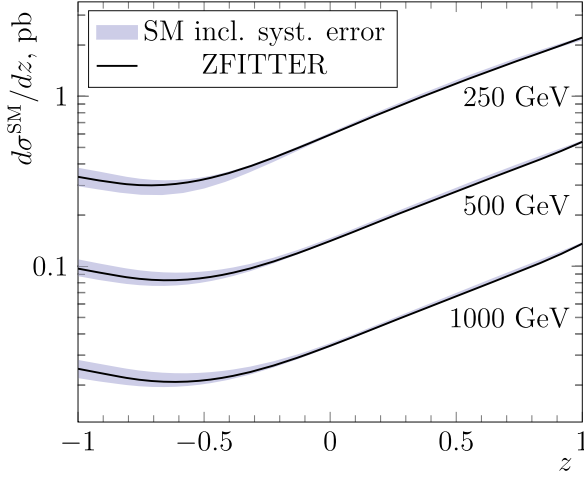


FIG. 1. The SM differential cross section (unpolarized) in picobarns with 2% systematical error used in numeric calculations. The results of ZFITTER are plotted as lines.

with

$$f(s, x, y) = x^2(1 - \epsilon)(3 + \epsilon) + (y + \epsilon x)^2 \frac{s}{s - M_Z^2}, \quad (5)$$

where θ_W is the Weinberg angle and $\epsilon = 1 - 4 \sin^2 \theta_W$. The small parameter ϵ is less than a few percent at the considered center-of-mass energies, so it can be set to zero in qualitative analysis. Since both the Z' couplings a' and v' are of the same order, the contribution of the first term in f is approximately 2.5–3 times larger than the contribution from the second term (at the ILC energies). So, the second argument in f dominates over the third argument. This means that

- (i) the z -odd part of F_1 is mainly related to the axial-vector Z' coupling a'_e ;
- (ii) the z -even part of F_1 is mainly related to the vector Z' coupling v'_e ;
- (iii) the factor F_1 weakly depends on the collision energy.

The next-to-leading-order (NLO) factor F_2 in (2) is mainly determined by the squared amplitude with an intermediate Z' state. Its improved Born approximation is

$$F_2(s, z, a', v') = \frac{g_{Z'}^4 s}{32\pi M_Z^4} \times [8a_e'^2 v_e'^2 z + (a_e'^2 + v_e'^2)^2 (1 + z^2)]. \quad (6)$$

To estimate the NLO contribution to the cross section, we compare F_1 and μF_2 at the highest ILC energy (1 TeV) and the lowest Z' mass (4 TeV). The corresponding value of the expansion parameter $\mu = -6.7 \times 10^{-4}$. These settings give the maximal possible contribution beyond the LO. The comparison between F_1 and μF_2 is shown in Fig. 2, in which the lines cover different values of z . The dots show the maximal values of F_1 (at $z = 1$) used to set the level of

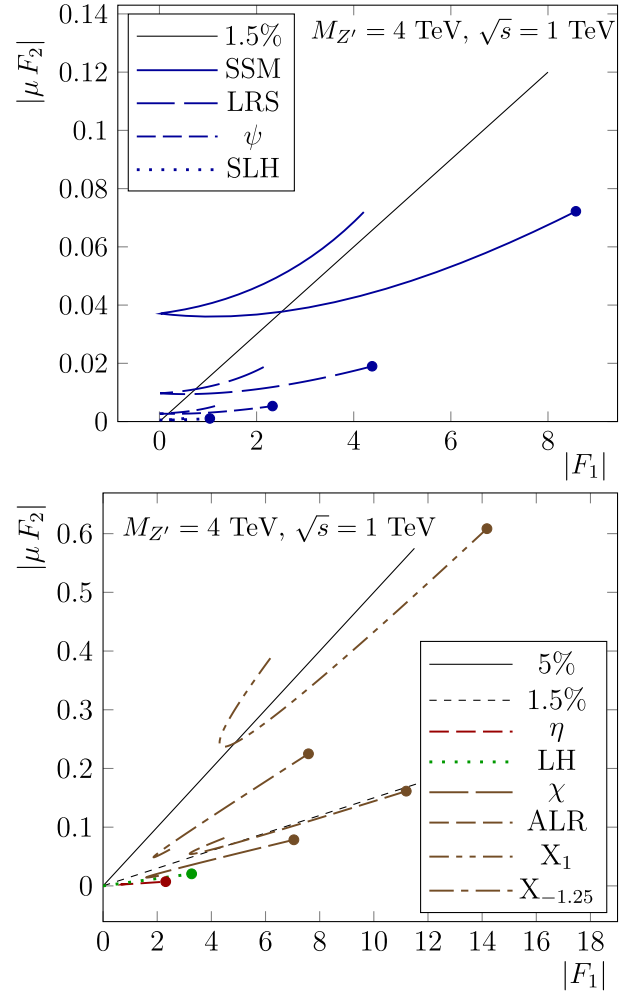


FIG. 2. Estimation of the NLO contribution in μ to the cross section. The Z' mass and the collision energy correspond to the maximal influence from F_2 , $\mu = -6.7 \times 10^{-4}$. The dots show the maximal values of F_1 used to set the level of systematic errors. In $U(1)_{X,x=1}$ and $U(1)_{X,x=-1.25}$ models (marked as X_1 and $X_{-1.25}$), the NLO term is below 4% of F_1 . For other models, this term is below 1.5%. Lower energies and higher $M_{Z'}$ suppress the relative contribution from F_2 . The plotted factors for the $U(1)_X$ model must be multiplied by 2.5. The factors are in picobarns.

systematic errors. In the $U(1)_{X,x=1}$ and $U(1)_{X,x=-1.25}$ models, the NLO term is below 4% of the leading term. For other models, it is below 1.5%. Of course, energies below 1 TeV and $M_{Z'} > 4$ TeV give smaller relative contributions from F_2 .

The fine structure constant α_{em} is determined by the photon polarization operator (see Fig. 3). The Weinberg angle is taken in accordance with Ref. [30], so it is higher than the value at the Z peak used, e.g., in Ref. [31]. The numeric values can be found in Table III. As is seen from Eq. (4), the systematic error from the fine structure constant is factorized and irrelevant for the angular behavior of the Z' factor. On the other hand, the systematic error of the Weinberg angle has to be taken into account during angular

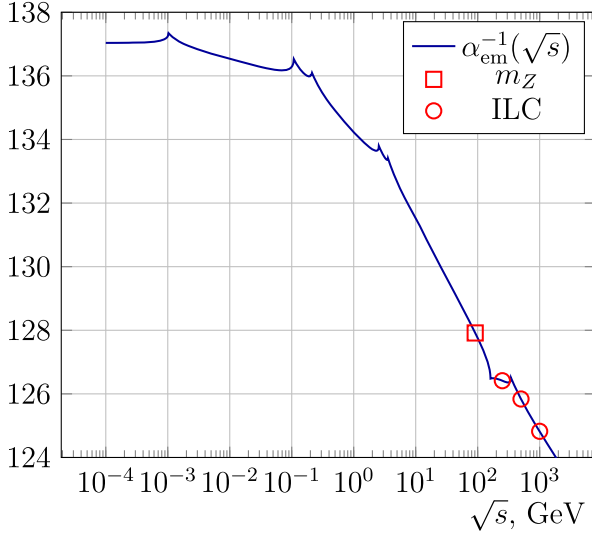


FIG. 3. The fine structure constant α_{em} determined by the photon polarization operator in a wide interval of energies. The values at m_Z as well as at the supposed ILC energies are shown separately.

integrations. We can estimate it by means of the first (leading) term in (5):

$$\left| \frac{\delta_{\text{syst}} F_1}{F_1} \right| \simeq \left| \frac{\delta_{\text{syst}} f}{f} \right| \simeq 0.7 |\delta_{\text{syst}} \epsilon|. \quad (7)$$

Comparing the values in Table III with the effective leptonic Weinberg angle at the Z peak ($\simeq 0.23$), we conclude that the nonfactorizable radiative corrections in F_1 are up to 4%. Thus, all the systematic errors (including radiative corrections and the expansion in μ) are estimated below 4%. In further calculations, we will use the LO factor F_1 and add the systematic error of order 5% of the maximal value of $F_1(z)$ to take into account effects beyond the approximation used.

The Z' factors in the models are shown in Fig. 4 for the center-of-mass energy 250 GeV only, since there are no dramatic changes in their shapes for higher energies. We can select four different groups of models:

- (i) *SSM*, ψ , *LRS* and *SLH*.—In these models, the Z' vector coupling to charged leptons is suppressed. This can be seen by substitution $s_W^2 \simeq 1/4$, $A = 0$, $\alpha \simeq \sqrt{2}$ in Table II. The $U(1)_X$ model with $x_H/x_\Phi = -1/3$ also belongs to this class. Thus, the Z' factors

TABLE III. The running couplings used to calculate the Z' contribution to the cross section.

	250 GeV	500 GeV	1 TeV
$1/\alpha_{\text{em}}$	126.414	125.839	124.823
$\sin^2 \theta_W$	0.2368	0.2407	0.2446

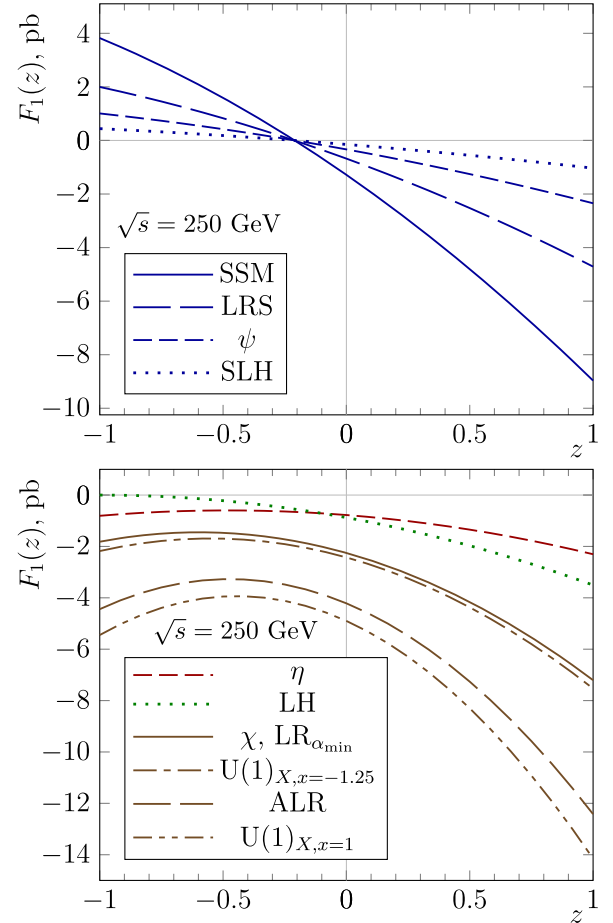


FIG. 4. The unpolarized factors $F_1(\sqrt{s}, z)$ in picobarns for models at 250 GeV. The factors are calculated up to 5% systematic error. The plotted factors for the $U(1)_X$ model must be multiplied by 2.5.

depend mainly on the axial-vector coupling and, consequently, on the z -odd term in (5). The factors are approximately proportional and odd with respect to z , so one could naively expect that the best signal would be described by the forward-backward cross section.

- (ii) η .—The suppressed Z' axial-vector coupling to charged leptons is a feature of the model. The axial-vector coupling vanishes exactly at $A = -B$ in Table II [$\beta = \arctan(-\sqrt{3/5}) \simeq -0.21\pi$]. For the η model, $\beta = \arctan(-\sqrt{5/3}) \simeq -0.29\pi$, and $A \simeq -B$. The Z' factor depends mainly on the vector coupling and, consequently, on the z -even term in (5). One could naively expect that the best signal would be described by the total cross section.
- (iii) *LH*.—The vector and the axial-vector couplings to charged leptons are equal. This means interactions with the left-handed chiral states only. The E_6 model with $A = B$ ($\beta = \arctan \sqrt{3/5}$, the so-called I model), the LR model with $\alpha = 1$, and the $U(1)_X$

model with $x_H/x_\Phi = -1/4$ also belong to this class. The angular dependence in this case is $F \sim (1+z)^2$, so the factor contains a dominant contribution from the forward scattering angles. One could naively expect that the best signal would be described by the forward cross section.

- (iv) χ , $\text{LR}_{\alpha_{\min}}$, $\text{U}(1)_{X,x=-1.25}$, ALR , $\text{U}(1)_{X,x=1}$.—These models show mixed angular dependence of the Z' factor.

As we will see in the next section, naive expectations about observables to amplify Z' signals do not correspond to the best choice. This is because the statistical error is not uniform over the scattering angle and has to be also taken into consideration to find the strongest signal of the particle.

III. OPTIMAL OBSERVABLE

The optimal observable to select the Z' signal is defined by weighted integration of the cross section,

$$\mathcal{I} = \int_{\Omega} dz w(z) \frac{d\sigma}{dz}, \quad (8)$$

where $w(z)$ is the weight function and Ω is the interval of available scattering angles. The complete phase space is given by $z \in [-1, 1]$. We will specify Ω when it influences the result.

The standard deviation of the observable can be calculated from the Poisson distribution of events (see Ref. [5]),

$$\delta\mathcal{I} \simeq \sqrt{\frac{1}{\mathcal{L}_{\text{eff}}} \int_{\Omega} dz w^2(z) \frac{d\sigma^{\text{SM}}}{dz}}. \quad (9)$$

where \mathcal{L} is the luminosity, and the cross section is substituted by its SM part, since the Z' contribution is tiny and leads to higher-order corrections in the inverse Z' mass. The SM cross section can be redefined to take into account the acceptance rate of events. We introduce the “effective” luminosity corrected by the polarization of the input beams: $\mathcal{L}_{\text{eff}} = (1 + P^+ P^-) \mathcal{L}$. In numeric estimates, the following integrated luminosities in inverse femtobarns are assumed: $\mathcal{L}_{250 \text{ GeV}} = 250 \text{ fb}^{-1}$, $\mathcal{L}_{500 \text{ GeV}} = 500 \text{ fb}^{-1}$, and $\mathcal{L}_{1 \text{ TeV}} = 1000 \text{ fb}^{-1}$ [1]. The polarizations of the initial electron and positron states are $P^- = \eta_{e_L^-} - \eta_{e_R^-}$ and $P^+ = \eta_{e_R^+} - \eta_{e_L^+}$, where η is the fraction of the corresponding particles. The definition of polarization is in accordance with Ref. [31].

The optimal observable satisfies the condition

$$\frac{\text{abs(signal)}}{\text{uncertainty}} = \frac{\text{abs}(\mathcal{I} - \mathcal{I}^{\text{SM}})}{\delta\mathcal{I}} \rightarrow \max, \quad (10)$$

where the Z' signal is the deviation from the SM; i.e., the SM is considered the background. The uncertainty is the statistical error (the standard deviation of the observable). This condition is actually a functional of the weight function w . Its maximum in the Hilbert space of w determines uniquely the weight function and the optimal observable.

In the considered Z' models, the theoretical prediction of the signal is

$$\mathcal{I} - \mathcal{I}^{\text{SM}} \simeq \mu \int_{\Omega} dz w(z) F_1(z). \quad (11)$$

As is seen, the unknown parameter factorizes, and the weight function is *independent of* μ :

$$\text{abs} \left[\frac{\int_{\Omega} dz w(z) F_1(z)}{\sqrt{\int_{\Omega} dz w^2(z) \frac{d\sigma^{\text{SM}}}{dz}}} \right] \rightarrow \max. \quad (12)$$

The target functional (12) is quite simple, and the exact analytic solution can be written. Since the SM cross section is strictly positive, let us define the following scalar product in the Hilbert space:

$$\langle f_1, f_2 \rangle = \int_{\Omega} dz f_1(z) f_2(z) \frac{d\sigma^{\text{SM}}}{dz}. \quad (13)$$

Then, the denominator of Eq. (12) is just the norm of the weight function, $\|w\|$, whereas the numerator is the scalar product between w and the function

$$\tilde{F}(z) = \frac{F_1(z)}{d\sigma^{\text{SM}}/dz}. \quad (14)$$

The function \tilde{F} does not depend on w . Dividing Eq. (12) by $\|\tilde{F}\|$, we obtain

$$\text{abs} \left[\frac{\langle w, \tilde{F} \rangle}{\|w\| \cdot \|\tilde{F}\|} \right] \rightarrow \max. \quad (15)$$

Thus, the target functional is the cosine between vectors w and \tilde{F} , and we immediately write the solution (up to a normalization factor C):

$$w(z) = C \tilde{F}(z) = C \frac{F_1(z)}{d\sigma^{\text{SM}}/dz}. \quad (16)$$

This solution reproduces exactly the general theory of the optimal observables [6–8]. We have additionally confirmed the result by numeric optimization described in details in Ref. [5], but the numeric approach contains no interesting details concerning the subject of the present paper to discuss it here. We have also cross-checked that the exact

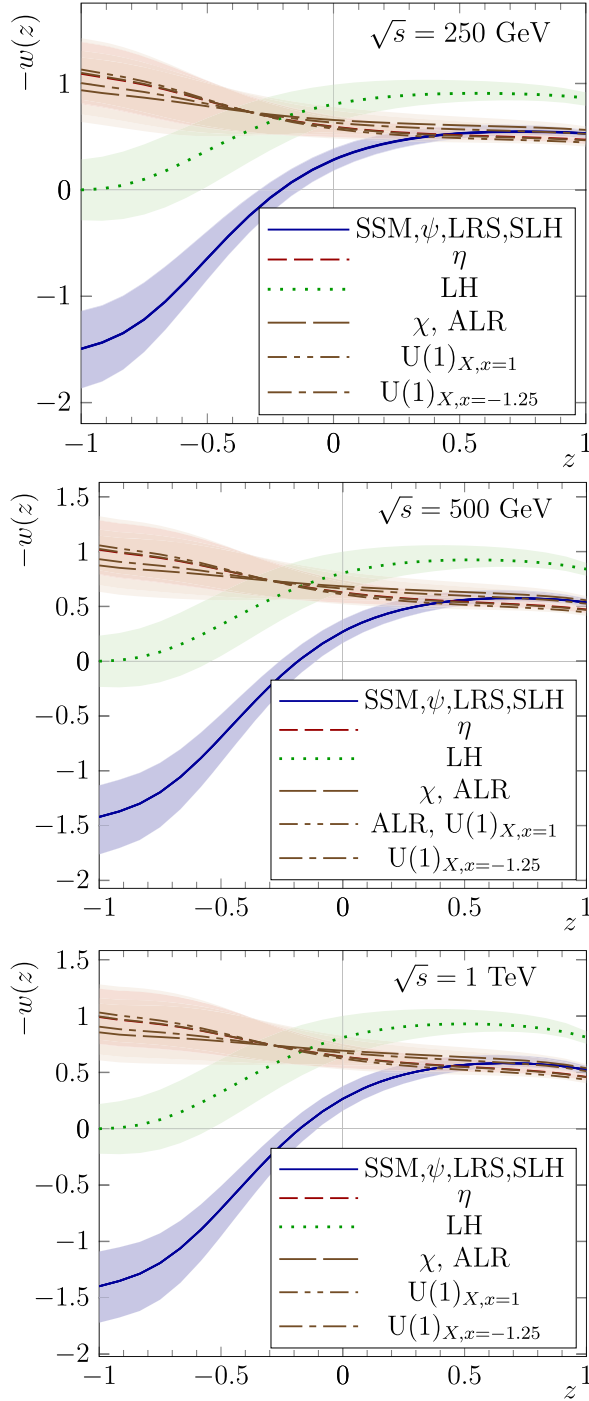


FIG. 5. The weight functions $-w(\sqrt{s}, z)$ to amplify the Z' signal and to measure $M_{Z'}$ at the ILC energies. The uncertainty arises from the systematic errors on the SM cross section and Z' factors. The universal normalization $\int_{-1}^1 w^2 dz = 1$ is used to compare different models. The negative sign at w is chosen to obtain positive values at $z = 1$. The actual systematic error might be significantly less, accounting for possible destructive interference between the weight function and the uncertainties of the SM and Z' contribution to the cross section. The lines correspond to the SM from ZFITTER.

solution (16) describes the numeric results obtained in Ref. [5].

To compare different Z' models, it is convenient to set the universal normalization of the weight function:

$$\int_{-1}^1 w^2 dz = 1, \quad C = \frac{1}{\sqrt{\int_{-1}^1 \left[\frac{F_1(z)}{d\sigma^{\text{SM}}/dz} \right]^2 dz}}. \quad (17)$$

The universally normalized weight functions are plotted in Fig. 5. As is seen, the weight functions are stable with respect to systematic errors and weakly depend on the center-of-mass energy. In the computation of systematic errors, possible destructive interference between the weight function and the uncertainties of the SM and Z' factor is not taken into account. So, the actual systematic error might be less by up to several times. Of course, more accurate calculation of the cross section could also reduce the error.

Some remnants of the “naive observables” for the Z' signal can be still found in the weight functions. For the SSM-like pool of models, we see the smoothed forward-backward cross section, but the weight function is not the step function anymore. In the LH model, the observable selects mainly the forward bins ($z \geq -0.5$). Other models are closer to the total cross section with increased weight of backward scattering angles.

IV. RELATION TO THE χ^2 FIT OF THE DIFFERENTIAL CROSS SECTION

Let us consider the fit of the Z' mass from the differential cross section. The observed events are aggregated into bins. Each bin is described by the following quantities:

- (i) Δz_i is the width of the i th bin.
- (ii) $\sigma_i, \sigma_i^{\text{SM}}$ are the observed cross section integrated in the bin and the correspondent SM value:

$$\sigma_i \simeq \left(\frac{d\sigma}{dz} \right)_{z_i} \Delta z_i.$$

- (iii) δ_i is the statistical error in the bin. In accordance with the Poisson distribution of events,

$$\delta_i^2 \simeq \mathcal{L}^{-1} \sigma_i \simeq \mathcal{L}^{-1} \sigma_i^{\text{SM}}.$$

- (iv) $F_{1,i}$ is the Z' factor integrated in the bin:

$$F_{1,i} \simeq F_1(z_i) \Delta z_i.$$

The χ^2 function is

$$\chi^2(\mu) = \sum_i \left(\frac{\sigma_i - \sigma_i^{\text{SM}} - \mu F_{1,i}}{\delta_i} \right)^2. \quad (18)$$

The minimum of χ^2 can be found explicitly. It gives the maximum likelihood (ML) estimate of the parameter:

$$\mu_{\text{ML}} = \frac{\sum_i \frac{(\sigma_i - \sigma_i^{\text{SM}}) F_{1,i}}{\delta_i^2}}{\sum_i \frac{F_{1,i}^2}{\delta_i^2}}. \quad (19)$$

In the continuous limit,

$$\mu_{\text{ML}} = \int_{\Omega} dz w_{\text{ML}}(z) \left(\frac{d\sigma}{dz} - \frac{d\sigma^{\text{SM}}}{dz} \right),$$

$$w_{\text{ML}}(z) = \frac{\frac{F_1(z)}{d\sigma^{\text{SM}}/dz}}{\int_{\Omega} dz \frac{F_1^2(z)}{d\sigma^{\text{SM}}/dz}}. \quad (20)$$

As is seen, the ML estimate is described by the same weight function as the optimal observable described in the previous section. The only difference is the normalization of $w(z)$, which is not arbitrary in this case. The normalization condition can be written as follows:

$$\int_{\Omega} dz w_{\text{ML}}(z) F_1(z) = 1. \quad (21)$$

Thus, the weight function in Fig. 5 must be rescaled to be used as the ML estimator of the Z' mass. The corresponding conversion constants are summarized in Table IV. For realistic detectors, some cuts occur for the scattering angle near the beam direction. In this case, the conversion constant is larger, since the weight function is distributed over a smaller volume. Note that the shape of the weight function (up to the normalization factor) does not depend on the cuts in accordance with Eq. (16).

The χ^2 function also allows us to derive the confidence interval for the Z' mass. It is given by

$$\chi^2(\mu) - \chi_{\text{min}}^2 < \chi_{1,\text{CL}}^2 = N_{\text{CL}}^2, \quad (22)$$

where N_{CL} is the symmetric confidence level (CL) for the standard normal distribution; the interval $[-N_{\text{CL}}, N_{\text{CL}}]$ corresponds to probability p_{CL} . In other words, N_{CL} is the CL measured in units of the standard deviation (in the so-called sigmas). The χ^2 distribution with 1 degree of freedom is used, since a single linear parameter appears in the fit.

Calculating (22) explicitly, we obtain the confidence interval for μ :

$$(\mu - \mu_{\text{ML}})^2 \sum_i \frac{F_{1,i}^2}{\delta_i^2} < N_{\text{CL}}^2. \quad (23)$$

Taking one standard deviation, $N_{\text{CL}} = 1$, we derive the statistical error of the Z' signal:

TABLE IV. The conversion constants in inverse picobarns to obtain weight functions w_{ML} for the ML estimator (20), (43) from the weight functions normalized as $\int_{-1}^1 w^2 dz = 1$ (plotted in Fig. 5). The SM from ZFITTER is assumed. The complete phase space and realistic kinematic cuts are considered.

	250 GeV	500 GeV	1 TeV
$z \in [-1, 1]$			
SSM	0.229 335	0.223 967	0.222 132
χ	0.255 427	0.251 687	0.248 24
ψ	0.876 493	0.839 409	0.817 898
η	0.782 297	0.750 646	0.729 826
LRS	0.436 601	0.432 227	0.434 998
ALR	0.144 713	0.146 662	0.150 483
LH	0.5007	0.524 721	0.535 442
SLH	1.9879	1.895 37	1.835 67
$U(1)_{\chi,x=1}$	0.050 278 9	0.048 122 9	0.046 780 4
$U(1)_{\chi,x=-1.25}$	0.097 267 3	0.093 882 5	0.091 362 6
$z \in [-0.9848, 0.9848], (10^\circ < \theta < 170^\circ)$			
SSM	0.237 948	0.232 167	0.230 131
χ	0.261 228	0.257 191	0.253 523
ψ	0.909 494	0.870 178	0.847 366
η	0.800 892	0.767 772	0.746 045
LRS	0.452 973	0.448 038	0.450 659
ALR	0.148 165	0.150 018	0.153 834
LH	0.512 453	0.536 649	0.547 246
SLH	2.062 56	1.964 77	1.901 78
$U(1)_{\chi,x=1}$	0.0514 954	0.049 240 2	0.047 839 4
$U(1)_{\chi,x=-1.25}$	0.099 511 7	0.095 963 4	0.093 332 3

$$\delta_\mu = \text{abs}(\mu_{N_{\text{CL}}=1} - \mu_{\text{ML}}) = 1 / \sqrt{\sum_i \frac{F_{1,i}^2}{\delta_i^2}}. \quad (24)$$

We can also calculate the quality of the Z' signal. The signal means that $\mu = 0$ is excluded at some CL. Taking $\mu = 0$ in Eq. (23), we obtain

$$N_{\text{CL},\text{signal}} = |\mu_{\text{ML}}| \sqrt{\sum_i \frac{F_{1,i}^2}{\delta_i^2}} = \frac{|\mu_{\text{ML}}|}{\delta_\mu} \quad (25)$$

or, in the continuous limit,

$$N_{\text{CL},\text{signal}} = |\mu_{\text{ML}}| \sqrt{\mathcal{L} \int_{\Omega} dz \frac{F_1^2(z)}{d\sigma^{\text{SM}}/dz}}. \quad (26)$$

The right-hand side of Eq. (25) is just the signal-to-uncertainty ratio (10). In accordance with the previous section, it is maximal for the considered fit. Thus, the χ^2 fit of the differential cross section coincides again with the optimal observable, since both the approaches are actually the same ML estimate. It is well known that the ML fit is a sort of estimate with the best statistical efficiency.

TABLE V. The expected signal-to-uncertainty ratio $N_{\text{CL,signal}} = \frac{\mathcal{L} - \mathcal{L}^{\text{SM}}}{\delta \mathcal{L}}$ corresponding to the optimal observables at $M_{Z'} = 4$ TeV and the canonical ILC integrated luminosities 250, 500, and 1000 fb^{-1} for 0.25, 0.5, and 1 TeV.

	250 GeV	500 GeV	1 TeV
	$z \in [-1, 1]$		
SSM	1.50	4.31	12.92
χ	1.24	3.60	10.93
ψ	0.39	1.15	3.51
η	0.44	1.29	3.95
LRS	0.79	2.23	6.59
ALR	2.38	6.62	19.19
LH	0.50	1.40	4.13
SLH	0.17	0.51	1.56
$U(1)_{X,x=1}$	6.97	20.48	62.80
$U(1)_{X,x=-1.25}$	3.36	9.88	30.33
	$z \in [-0.9848, 0.9848], (10^\circ < \theta < 170^\circ)$		
SSM	1.48	4.23	12.69
χ	1.23	3.56	10.81
ψ	0.39	1.13	3.45
η	0.43	1.27	3.90
LRS	0.77	2.19	6.48
ALR	2.35	6.54	18.98
LH	0.49	1.38	4.08
SLH	0.17	0.50	1.54
$U(1)_{X,x=1}$	6.88	20.25	62.10
$U(1)_{X,x=-1.25}$	3.32	9.78	30.01

The expected signal-to-uncertainty ratio $N_{\text{CL,signal}}$ is shown in Table V for $M_{Z'} = 4$ TeV and the ILC canonical luminosities (250, 500, and 1000 fb^{-1} for 0.25, 0.5, and 1 TeV). It is easy to obtain this ratio for other Z' masses and luminosities, since $N_{\text{CL,signal}} \sim \sqrt{\mathcal{L}}/(s - M_{Z'}^2)$. The condition $N_{\text{CL,signal}} > 5$ means the discovery of the particle.

V. EFFECTS OF Z - Z' MIXING

The Z - Z' mixing angle θ_0 arises from the diagonalization of the mass matrix of neutral vector bosons. For a bunch of Z' models, it was discussed in details in Ref. [32]. In general, θ_0 depends on the couplings and the vacuum expectation values of scalar fields responsible for the spontaneous breakdown of gauge symmetries. Because of different possibilities to introduce the scalar sector, additional parameters like the ratios of vacuum expectation values occur, and the mixing angle cannot be reduced to the couplings in Table II exclusively. So, it has to be considered as a free parameter in the Z' models.

The Z - Z' mixing angle θ_0 can be written in the form

$$\theta_0 = C \frac{g_{Z'}}{g_Z} \frac{M_Z^2}{M_{Z'}^2}. \quad (27)$$

where $C \sim 1$ is a model-dependent factor. Explicit factors C can be found in Ref. [32].

In the presence of Z - Z' mixing, the Lagrangian (1) becomes more complicated. Namely, the Z and Z' couplings must be substituted by

$$\begin{aligned} g_Z v_f &\rightarrow g_Z v_f \cos \theta_0 + g_{Z'} v'_f \sin \theta_0, \\ g_Z a_f &\rightarrow g_Z a_f \cos \theta_0 + g_{Z'} a'_f \sin \theta_0, \\ g_{Z'} v'_f &\rightarrow g_{Z'} v'_f \cos \theta_0 - g_Z v_f \sin \theta_0, \\ g_{Z'} a'_f &\rightarrow g_{Z'} a'_f \cos \theta_0 - g_Z a_f \sin \theta_0. \end{aligned} \quad (28)$$

Since both the parameters θ_0 and μ behave like $\sim M_{Z'}^{-2}$, only the linear in θ_0 term in the cross section could correct the results from the previous sections:

$$\frac{d\sigma}{dz} \simeq \frac{d\sigma^{\text{SM}}}{dz} + \mu F_1(s, z, a', v') + \theta_0 F_{\text{mix}}(s, z, a', v'). \quad (29)$$

Let us notice that the current constraint on θ_0 ($\leq 10^{-4}$) means $\theta_0 \leq \mu$ for the ILC energies. Using the same notations as in Eqs. (4) and (6), we can write F_{mix} in the form

$$\begin{aligned} F_{\text{mix}}(s, z, a', v') &= -\frac{\alpha_{\text{em}}^{3/2} g_{Z'} \sqrt{\pi}}{32 \sin^3 \theta_W \cos^3 \theta_W (s - M_Z^2)} \\ &\times \left\{ z f_{\text{mix}}[s, a'_e, 2\epsilon(v'_e + a'_e \epsilon)] \right. \\ &\left. + \frac{1+z^2}{2} f_{\text{mix}}[s, v'_e \epsilon, (a'_e + v'_e \epsilon)(1 + \epsilon^2)] \right\}, \end{aligned} \quad (30)$$

with

$$f_{\text{mix}}(s, x, y) = x(1 - \epsilon)(3 + \epsilon) + y \frac{s}{s - M_Z^2}. \quad (31)$$

For qualitative analysis, the small parameter ϵ can be omitted:

$$F_{\text{mix}} \sim \left[z f_{\text{mix}}(s, a'_e, 0) + \frac{1+z^2}{2} f_{\text{mix}}(s, 0, a'_e) \right]. \quad (32)$$

As is seen, the contribution from the Z - Z' mixing is related to the axial-vector coupling. This fact is explained as follows. In the SM, the Z vector coupling to charged leptons is suppressed (it is $\sim \epsilon$; see the SSM couplings with $s_W^2 \simeq 1/4$). On the other hand, only the Z exchange Feynman diagram contributes to F_{mix} (the Z' exchange Feynman diagram $\sim \mu \epsilon$).

To estimate effects from Z - Z' mixing, let us compare Eq. (32) with Eq. (4). First of all, for $v'_e = 0$, both the factors F_1 and F_{mix} contain the same angular dependency (up to ϵ^2). This means that in the models with suppressed vector coupling v'_e the mixing angle corrects the estimated parameter μ and cannot be separated in the leading order in $M_{Z'}^{-2}$. Thus, for the SSM, LRS, ψ , and SLH models, all the

TABLE VI. The effective parameter μ^* in the models with suppressed v'_e .

	250 GeV	500 GeV	1 TeV
SSM	$\mu - 0.31\theta_0$	$\mu - 0.07\theta_0$	$\mu - 0.02\theta_0$
LRS	$\mu + 0.42\theta_0$	$\mu + 0.09\theta_0$	$\mu + 0.02\theta_0$
ψ	$\mu + 0.60\theta_0$	$\mu + 0.13\theta_0$	$\mu + 0.03\theta_0$
SLH	$\mu + 0.90\theta_0$	$\mu + 0.20\theta_0$	$\mu + 0.05\theta_0$

results from the previous sections remain unchanged after updating μ :

$$\mu \rightarrow \mu^* = \mu + \theta_0 \frac{\sqrt{\pi\alpha} M_Z^2}{a'_e g_{Z'} \sin\theta_W \cos\theta_W (M_Z^2 - s)}. \quad (33)$$

The effective parameter μ^* is shown in Table VI for different ILC energies. In what follows, we will ignore these models discussing the Z - Z' mixing.

Second, in the models with suppressed axial-vector coupling $a'_e \simeq 0$, the Z - Z' mixing may be ignored. Indeed, in accordance with (32), $\theta_0 \simeq 0$. The model from the considered list closest to this case is the η model.

The factors in the cross section have universal behavior with respect to the collision energy:

$$F_{\text{mix}} \sim s^{-1}, \quad F_1 \sim \text{const}, \quad M_Z \ll \sqrt{s} < M_{Z'}.$$

F_{mix} is less than 2.5% of F_1 at $\sqrt{s} = 1$ TeV. For $\sqrt{s} = 500$ GeV, it exceeds 5% of F_1 only for the LH model. These magnitudes are comparable with the systematic error for F_1 , so Z - Z' mixing does not influence the results obtained in the previous sections for $\sqrt{s} \geq 500$ GeV.

The angular dependence $F_{\text{mix}}(z)$ is shown in Fig. 6. The odd shape is not surprising, since the effects of Z - Z' mixing cannot be separated from F_1 in the models with odd F_1 .

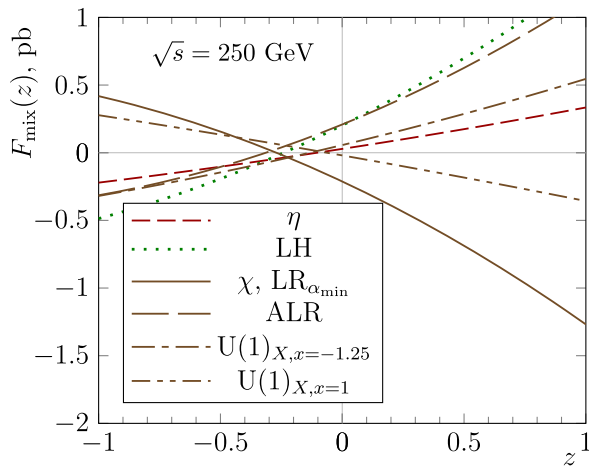


FIG. 6. The unpolarized factors $F_{\text{mix}}(\sqrt{s}, z)$ in picobarns at 250 GeV for the models with the mixing angle as a separate parameter. The factors are calculated up to 5% systematic error. The plotted factors for the $U(1)_X$ model must be multiplied by 2.5.

Visible effects of Z - Z' occur at the lower ILC energy $\sqrt{s} = 250$ GeV only. In this case, there are optimal observables to select either μ or θ_0 . The easiest way to derive them is either to adopt general formulas from Refs. [6,7] or to write the χ^2 fit with several parameters. Let us denote the set of fitted parameters as γ_i , the corresponding factors in the differential cross section as F_i , and the weight function as w_i . In our case,

$$\begin{aligned} \gamma_i &= [\mu, \theta_0], \\ F_i &= [F_1, F_{\text{mix}}], \\ w_i &= [w_\mu, w_{\theta_0}]. \end{aligned} \quad (34)$$

The result is

$$\begin{aligned} \gamma_{i,\text{ML}} &= \int_{\Omega} dz w_{i,\text{ML}}(z) \left(\frac{d\sigma}{dz} - \frac{d\sigma^{\text{SM}}}{dz} \right), \\ w_{i,\text{ML}} &= \sum_j \tilde{c}_{ij}^{-1} \frac{F_j(z)}{d\sigma^{\text{SM}}/dz}, \end{aligned} \quad (35)$$

where \tilde{c}_{ij}^{-1} is the inverse matrix for

$$\tilde{c}_{ij} = \int_{\Omega} dz \frac{F_i(z) F_j(z)}{d\sigma^{\text{SM}}/dz}. \quad (36)$$

The numerical values of \tilde{c}_{ij}^{-1} are given in Table VII. It is easy to see that Eq. (35) gives Eq. (20) for the single parameter μ .

TABLE VII. The numeric values of matrix \tilde{c}_{ij}^{-1} in inverse picobarns. The complete phase space is suggested ($z \in [-1, 1]$).

	\tilde{c}_{11}^{-1}	\tilde{c}_{12}^{-1}	\tilde{c}_{22}^{-1}
250 GeV			
χ	0.057 661 7	-0.176493	2.322 41
η	0.355 642	-0.0730611	13.4809
ALR	0.015 201 2	0.097 004	2.975 55
LH	0.631 465	1.142	3.64662
$U(1)_{X,x=1}$	0.001 439 55	0.007 556 2	1.539 29
$U(1)_{X,x=-1.25}$	0.006 093 76	0.008 429 94	0.956 269
500 GeV			
χ	0.013 021 3	-0.157882	11.0761
η	0.084 174 5	0.054 396 4	63.7052
ALR	0.003 678 1	0.083 681 2	14.2823
LH	0.149 855	1.1523	16.9333
$U(1)_{X,x=1}$	0.000 334 045	0.003 702 35	7.177 84
$U(1)_{X,x=-1.25}$	0.001 457 13	0.011 784 5	4.567 11
1 TeV			
χ	0.002 961 17	-0.131345	44.4095
η	0.019 889 5	0.206 536	254.214
ALR	0.000 909 918	0.065 510 9	56.9887
LH	0.035 551 7	1.082 69	67.0021
$U(1)_{X,x=1}$	0.000 077 959 9	-0.000906613	28.3105
$U(1)_{X,x=-1.25}$	0.000 346 823	0.015 299 9	18.4215

In terms of the Hilbert space from Sec. III,

$$\tilde{c}_{ij} = \left\langle \frac{F_i}{d\sigma^{\text{SM}}/dz}, \frac{F_j}{d\sigma^{\text{SM}}/dz} \right\rangle, \quad (37)$$

$$\left\langle w_{i,\text{ML}}, \frac{F_j}{d\sigma^{\text{SM}}/dz} \right\rangle = \begin{cases} 1, & i = j, \\ 0, & i \neq j. \end{cases}$$

The last equation corresponds to Eq. (21). First of all, it means that the weight function for a given parameter must be orthogonal to all the remaining Z' factors in the differential cross section,

$$\int_{\Omega} dz w_{i,\text{ML}}(z) F_{j \neq i}(z) = 0. \quad (38)$$

With this projection of F_i to the axis orthogonal to any other factor, we obtain the result exactly corresponding to the one-dimensional optimization from Sec. III. This is the definition of the optimal observable through *conditional maximization of the signal-to-uncertainty ratio* (10) with the additional constraints to exclude contributions from other unknown parameters [5].

The weight functions to measure separately μ and θ_0 at $\sqrt{s} = 250$ GeV are shown in Fig. 7. If the weight function for μ is close to the total cross section in the absence of the Z - Z' mixing, we see no qualitative changes of the shape of w_{μ} with θ_0 taken into account. This can be explained by the fact that such models have initially approximately orthogonal factors F_1 (even) and F_{mix} (odd). However, the common tendency is the growing weight of the backward bins.

The weight function to measure the Z - Z' mixing angle always has an approximately odd shape. It is close to the weight function for μ^* in the models with suppressed vector coupling of the Z' boson to charged leptons.

For the models with the Z' couplings to left-handed chiral states of charged leptons only (the LH model), the situation becomes more interesting. In this case, we have three completely different optimal observables: two observables to measure μ with either the absence or presence of the Z - Z' mixing and one observable to measure the mixing angle. Their application to data would allow us to obtain a lot of information about the Z - Z' mixing angle.

Another possibility to account for the Z - Z' mixing is some model-independent definitions of θ_0 . For instance, let us consider the Abelian Z' boson [33] including, in particular, the χ , LR, and $U(1)_X$ models. In this case, there is a relation inspired by the renormalization group equations below the threshold of Z' decoupling:

$$\theta_0 \simeq \frac{2g_{Z'} a'_e \sin \theta_W \cos \theta_W}{\sqrt{2\pi\alpha_{\text{em}}}} \frac{M_Z^2}{M_{Z'}^2}. \quad (39)$$

The optimal observables to measure Abelian Z' couplings were discussed in Ref. [5]. It was also shown in Ref. [34] for the Abelian Z' boson that the mixing angle plays an

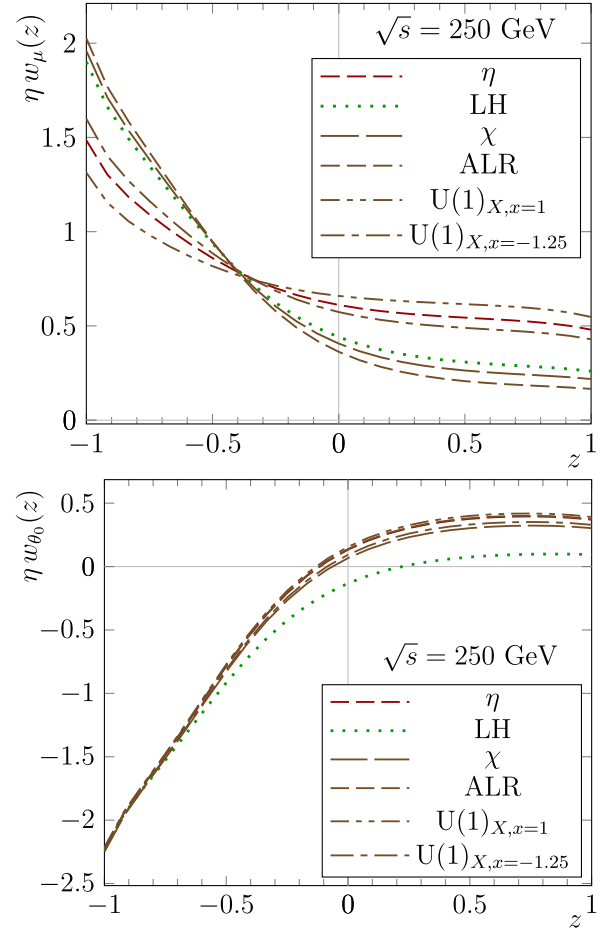


FIG. 7. The weight functions $\eta w(\sqrt{s}, z)$ to measure $M_{Z'}$ and θ_0 at the ILC energies. The universal normalization $\int_{-1}^1 w^2 dz = 1$ is used to compare different models. The sign $\eta = -1$ for the χ and $U(1)_{X,x=1}$ models and $\eta = 1$ otherwise. The lines correspond to the SM from ZFITTER. The complete phase space $z \in [-1, 1]$ is used.

important role in calculations at the Z' peak. Since θ_0 is expressed in terms of the Z' couplings, no additional parameters occur. However, factor F_1 has to be corrected to include contribution from the Z - Z' mixing:

$$F_1 \rightarrow F_1 - \frac{2g_{Z'} a'_e \sin \theta_W \cos \theta_W}{\sqrt{2\pi\alpha_{\text{em}}}} F_{\text{mix}}. \quad (40)$$

The corresponding weight functions are compared with the case of absent mixing in Fig. 8. As is seen, the mixing angle affects the weight function up to 10% at $\sqrt{s} = 250$ GeV. For higher collision energies, the contribution from θ_0 decreases essentially.

Finally, let us remind the reader that there is no chance to separate and measure the Z - Z' mixing angle in the models with suppressed vector Z' couplings to charged leptons (SSM, ψ , LRS, and SLH) nor for collision energies $\sqrt{s} \geq 500$ GeV within ILC experiments. Thus, the role of mixing is important at energies ~ 250 GeV.

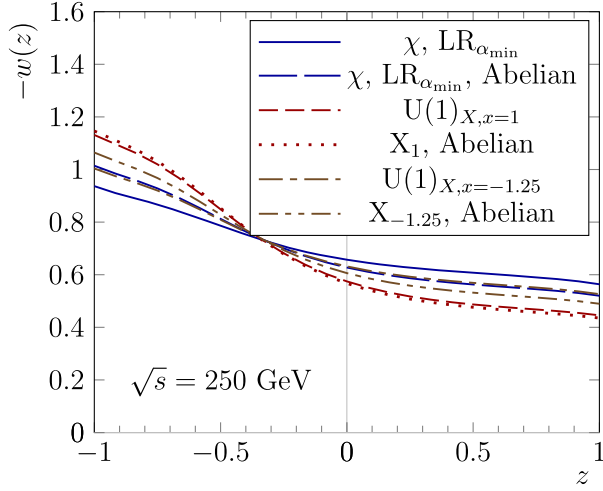


FIG. 8. The weight functions $-w(\sqrt{s}, z)$ to measure μ in the Abelian models with θ_0 from Eq. (39). The universal normalization $\int_{-1}^1 w^2 dz = 1$ is used to compare different models. The shorthand notations X_1 and $X_{-1.25}$ are used for $U(1)_{X,x=1}$ and $U(1)_{X,x=-1.25}$ models.

VI. DISCUSSION

In the paper, we have considered a set of popular Z' models in the annihilation leptonic process. We have investigated weighted integrated cross sections with the best ratio of the Z' signal to statistical uncertainty (the optimal observables). They uniquely define the weight of every event in the phase space of the final particles. Then, all the available events can be summed up with the weights without intermediate aggregation into bins with respect to the scattering angle. The CL of the signal corresponds to the highest possible level allowed by the integrated luminosity.

We have shown that the optimal observables are equivalent to the χ^2 fit of the differential cross section. In this regard, it is a unique integration scheme of the cross section that leads to no losses of information encoded in the differential cross section. The optimal observables can be implemented as a simple and convenient alternative to the complete analysis of the differential cross section: it could simply accumulate events from the start of an experiment without additional manipulation of data leading directly to the ML estimator for the Z' mass.

It is interesting to compare the estimates based on the optimal observables with the popular approach taking into consideration the forward-backward asymmetry A_{FB} . Such an analysis can explain a lot of details of application of A_{FB} within the Z' models. In Ref. [31], the 95% exclusion reaches for the Z' mass were calculated by means of A_{FB} assuming polarizations $P^- = 0.8, P^+ = 0.3$ at 0.5 TeV and $P^- = 0.8, P^+ = 0.2$ at 1 TeV. We choose the same settings and calculate exclusion reaches based on the optimal observables. First of all, substituting the deviation from the SM in (20) by the value predicted by the Z' model,

$$\frac{d\sigma}{dz} - \frac{d\sigma^{\text{SM}}}{dz} \simeq \frac{M_Z^2}{s - M_Z^2} F_1(z), \quad (41)$$

we obtain the obvious ML estimate of the model parameter (3). Then, specifying the 95% confidence level, $N_{\text{CL}} = 2$, and solving (26) for the Z' mass, we obtain the *exclusion reach*,

$$M_{Z',95\%}^2 \simeq s + \frac{M_Z^2}{2} \sqrt{\mathcal{L} \int_{\Omega} dz \frac{F_1^2(z)}{d\sigma^{\text{SM}}/dz}}, \quad (42)$$

since any lower value of the Z' mass will be detected as the signal at the considered CL.

In Table VIII, we compare the exclusion reaches from the optimal observables and from the forward-backward asymmetries [31]. We take the same interval of scattering angles $10^\circ < \theta < 170^\circ$, which corresponds to $z \in [-0.9848, 0.9848]$. The exclusion reaches from the optimal observables are always higher than in any other scheme, since this approach is more efficient from the statistical point of view. However, the difference is not uniform over the Z' models. In case of the SSM, ψ , and LRS models, the weight function is closer to the forward-backward integration scheme, so the exclusion reach increases up to 10%. Actually, the forward-backward asymmetry might be good to search for these models. On the other hand, the weight functions of the χ and η models are far away from odd shapes. The exclusion reaches from A_{FB} are weak in this case, and the forward-backward asymmetry seems to be insufficient to fit data. Indeed, the optimal observables increase the exclusion reaches up to 200%.

TABLE VIII. The exclusion reach on $M_{Z'}$ (TeV) at 95% CL from the optimal observable. The correspondent exclusion reach from the forward-backward asymmetry from Ref. [31] is also presented. The polarizations $P^- = 0.8, P^+ = -0.3$ at 500 GeV and $P^- = 0.8, P^+ = -0.2$ at 1 TeV are assumed. The results in Ref. [31] are rounded up to 0.5 TeV.

\sqrt{s}	250 GeV		500 GeV		1 TeV	
	Eq. (42)	Ref. [31]	Eq. (42)	Ref. [31]	Eq. (42)	Ref. [31]
SSM	3.4	5.5	5.8	9.8	9.8	9.8
ψ	1.8	2.7	3.0	4.7	5.2	5.2
LRS	2.5	3.7	4.2	6.5	7.0	7.0
SLH	1.2	...	2.0	...	3.5	3.5
χ	3.1	1.6	5.3	3	9.1	9.1
η	1.9	1.7	3.2	3	5.5	5.5
ALR	4.3	...	7.2	...	12.0	12.0
LH	2.0	...	3.3	...	5.6	5.6
$U(1)_{X,x=1}$	7.4	...	12.6	...	21.6	21.6
$U(1)_{X,x=-1.25}$	5.2	...	8.8	...	15.0	15.0

For a concluding remark, we note that the optimal observable shows the best fit of data. It allows us to obtain the ML estimator of the Z' mass, taking into account the distribution of events over the phase space of the final particles with no loss of information. The approach can be applied to treat experimental data even for small samples when the aggregation of events into a detailed differential cross section is practically impossible. Such a feature would be very useful at the start of experiment. Indeed, Eq. (20) can be rewritten as

$$\frac{1}{s - M_{Z',\text{ML}}^2} \simeq \sum_{i \in \text{events}} \frac{w_{\text{ML},i}}{M_Z^2 \mathcal{L}} - \int_{-1}^1 dz \frac{w_{\text{ML}}(z)}{M_Z^2} \frac{d\sigma^{\text{SM}}}{dz}, \quad (43)$$

where the sum runs over all the observed events, $w_{\text{ML},i}$ corresponds to the measured scattering angle, \mathcal{L} means the

actual luminosity taking into account the event acceptance rate, and the integral is the SM background calculated, for instance, by the event generator for the actual detector. Thus, the optimal observable can be considered as a technique of continuous accumulation of events with on the fly fit of the Z' mass from the implied differential cross section without actual construction of the differential cross section. No signal from the optimal observable would mean that there is no sense in further searching for the Z' model in the collected data.

Introducing the acceptance rates in the phase space and other minor technical improvements are beyond the scope of this paper. They could be revisited at the stage of practical implementation of the optimal observables at future lepton colliders.

-
- [1] H. Baer, T. Barklow, K. Fujii, Y. Gao, A. Hoang, S. Kanemura, J. List, H. E. Logan, A. Nomerotski, M. Perelstein *et al.*, The International Linear Collider technical design report—Volume 2: Physics, arXiv:1306.6352.
- [2] G. Weiglein *et al.* (LHC/LC Study Group), Physics interplay of the LHC and the ILC, *Phys. Rep.* **426**, 47 (2006).
- [3] M. Aaboud *et al.* (ATLAS Collaboration), Search for new high-mass phenomena in the dilepton final state using 36 fb⁻¹ of proton-proton collision data at $\sqrt{s} = 13$ TeV with the ATLAS detector, *J. High Energy Phys.* **10** (2017) 182.
- [4] A. M. Sirunyan *et al.* (CMS Collaboration), Search for high-mass resonances in dilepton final states in proton-proton collisions at $\sqrt{s} = 13$ TeV, *J. High Energy Phys.* **06** (2018) 120.
- [5] A. Gulov, Optimal one-parameter observables for the Z' in $e^+e^- \rightarrow \mu^+\mu^-$ process, *Int. J. Mod. Phys. A* **29**, 1450161 (2014).
- [6] D. Atwood and A. Soni, Analysis for magnetic moment and electric dipole moment form-factors of the top quark via $e^+e^- \rightarrow t\bar{t}$, *Phys. Rev. D* **45**, 2405 (1992).
- [7] M. Diehl and O. Nachtmann, Optimal observables for the measurement of three gauge boson couplings in $e^+e^- \rightarrow W^+W^-$, *Z. Phys. C* **62**, 397 (1994).
- [8] M. Diehl, O. Nachtmann, and F. Nagel, Triple gauge couplings in polarised $e^+e^- \rightarrow W^+W^-$ and their measurement using optimal observables, *Eur. Phys. J. C* **27**, 375 (2003).
- [9] G. Aad *et al.* (ATLAS Collaboration), Test of CP invariance in vector-boson fusion production of the Higgs boson using the Optimal Observable method in the ditau decay channel with the ATLAS detector, *Eur. Phys. J. C* **76**, 658 (2016).
- [10] J. L. Hewett and T. G. Rizzo, Low-energy phenomenology of superstring-inspired E_6 models, *Phys. Rep.* **183**, 193 (1989).
- [11] A. Leike, The phenomenology of extra neutral gauge bosons, *Phys. Rep.* **317**, 143 (1999).
- [12] T. G. Rizzo, in *Proceedings of Theoretical Advanced Study Institute in Elementary Particle Physics: Exploring New Frontiers Using Colliders and Neutrinos (TASI 2006)*, Boulder, Colorado, 2006 (World Scientific, Hackensack, USA, 2006), p. 537.
- [13] P. Langacker, The physics of heavy Z' gauge bosons, *Rev. Mod. Phys.* **81**, 1199 (2009).
- [14] F. Gursev, P. Ramond, and P. Sikivie, A universal gauge theory model based on E_6 , *Phys. Lett.* **60B**, 177 (1976).
- [15] J. C. Pati and A. Salam, Lepton number as the fourth "color", *Phys. Rev. D* **10**, 275 (1974); Erratum **11**, 703 (1975).
- [16] E. Ma, Particle dichotomy and left-right decomposition of E_6 superstring models, *Phys. Rev. D* **36**, 274 (1987).
- [17] M. Ashry and S. Khalil, Phenomenological aspects of a TeV-scale alternative left-right model, *Phys. Rev. D* **91**, 015009 (2015); Publisher's Note **96**, 059901 (2017).
- [18] N. Arkani-Hamed, A. G. Cohen, E. Katz, and A. E. Nelson, The Littlest Higgs, *J. High Energy Phys.* **07** (2002) 034.
- [19] T. Han, H. E. Logan, B. McElrath, and L.-T. Wang, Phenomenology of the little Higgs model, *Phys. Rev. D* **67**, 095004 (2003).
- [20] D. E. Kaplan and M. Schmaltz, The Little Higgs from a simple group, *J. High Energy Phys.* **10** (2003) 039.
- [21] I. C. Maldonado, A. F. Tellez, and G. Tavares-Velasco, Radiative decays $Z_H \rightarrow V_i Z (V_i = \gamma, Z)$ in little Higgs models, *J. Phys.* **39**, 015003 (2012).
- [22] S. Oda, N. Okada, and D.-s. Takahashi, Classically conformal $U(1)'$ extended standard model and Higgs vacuum stability, *Phys. Rev. D* **92**, 015026 (2015).
- [23] A. Das, S. Oda, N. Okada, and D.-s. Takahashi, Classically conformal $U(1)'$ extended standard model, electroweak vacuum stability, and LHC Run-2 bounds, *Phys. Rev. D* **93**, 115038 (2016).
- [24] K. A. Olive *et al.* (Particle Data Group), Review of Particle Physics, *Chin. Phys. C* **38**, 090001 (2014).

- [25] P. Osland, A. A. Pankov, and A. V. Tsytinov, Identification of extra neutral gauge bosons at the International Linear Collider, *Eur. Phys. J. C* **67**, 191 (2010).
- [26] T. Hahn, Generating Feynman diagrams and amplitudes with FeynArts 3, *Comput. Phys. Commun.* **140**, 418 (2001).
- [27] T. Hahn and M. Perez-Victoria, Automated one-loop calculations in four and D dimensions, *Comput. Phys. Commun.* **118**, 153 (1999).
- [28] D. Yu. Bardin and G. Passarino, *The Standard Model in the Making: Precision Study of the Electroweak Interactions* (Clarendon Press, Oxford, UK, 1999).
- [29] A. B. Arbuzov, M. Awramik, M. Czakon, A. Freitas, M. W. Grunewald, K. Monig, S. Riemann, and T. Riemann, ZFITTER: a semi-analytical program for fermion pair production in e^+e^- annihilation, from version 6.21 to version 6.42, *Comput. Phys. Commun.* **174**, 728 (2006).
- [30] J. Erler and M. J. Ramsey-Musolf, Weak mixing angle at low energies, *Phys. Rev. D* **72**, 073003 (2005).
- [31] T. Han, P. Langacker, Z. Liu, and L.-T. Wang, , Diagnosis of a new neutral gauge boson at the LHC and ILC for Snowmass 2013, [arXiv:1308.2738](https://arxiv.org/abs/1308.2738).
- [32] P. Langacker and M.-x. Luo, Constraints on additional Z' bosons, *Phys. Rev. D* **45**, 278 (1992).
- [33] A. V. Gulov and V. V. Skalozub, Renormalizability and model-independent description of Z' signals at low energies, *Eur. Phys. J. C* **17**, 685 (2000).
- [34] A. O. Pevzner, Influence of the $Z - Z'$ mixing on the Z' production cross section in the model-independent approach, *Nonlinear Phenom. Complex Syst.* **21**, 30 (2018).